Article ID: 1003 - 6326(2000)03 - 0378 - 04

Tensile properties and fracture behavior of Ti_2AlNb based alloys at room temperature ①

PENG Ji-hua(彭继华)[1,2], MAO Yong(毛 勇)[2], LI Shi-qiong(李世琼)[2], SUN Xun-fang(孙训方)[2]

1. *Department of Engineering Mechanics, Southwest Jiaotong University, Chengdu 610031, P. R. China;*

2. *Division of Super Alloys, Central Iron and Steel Research Institute, Beijing 100081, P. R. China*

Abstract: The tensile mechanical properties and fracture behaviors of Ti-22Al-20Nb-7Ta alloys were studied at room temperature. Three typical microstructures of Ti_2AlNb based alloys were obtained by combination of thermal mechanical processing and heat treat-ment. They are: 1) lath mixture of $O+B2$ with remaining β grain boundaries and α_2 phase; 2) equiaxed O phase in $B2$ matrix; 3) fine lath mixture of $O+B2$ without remaining β grain boundaries. It is shown that the microstructure obviously affects the tensile properties of Ti_2AlNb based alloys. The microstructure of fine lath mixture of $O+B2$ without remaining β grain boundaries has good combination of yield stress and ductility, while the microstructure with lath mixture of $O+B2$ with remaining β grain boundaries and α_2 phase has low yield stress and elongation. The fracture mode was also controlled by the microstructure of Ti_2AlNb based alloys. By means of SEM, it was found that the dominated fracture mode of microstructure with lath mixture of $O+B2$ with remained β grain boundary and α_2 phase was intergranular, and the fracture mode of the other two microstructures was mainly transgranular.

Key words: Ti_2AlNb based alloys; tensile properties; fracture behavior **Document code:** A

1 INTRODUCTION

The class of orthorhombic titanium aluminide alloys currently appears to offer excellent potential as aerospace and elevated temperature structural materials because of their low density and high strength[1,2]. The conventional Ti_3Al based alloy Ti-24Al-11Nb possesses higher toughness at room temperature, however, the balance combination of toughness, ductility at room temperature, and fracture strength, creep resistance at elevated temperature must be considered[3]. Ti-25Al-10Nb-1Mo has obtained higher creep resistance at the loss of room temperature toughness. TAC-1 alloy developed by the Central Iron and Steel Research Institute has improved the balance combination of mechanical properties for Ti_3Al based alloy, but its yield strength at room temperature is lower than 1 000 MPa[4]. Recently, Ti_3Al based alloys are going toward higher Nb content, and an orthorhombic phase (Ti_2AlNb) was found. It is intriguing that Ti_2AlNb based alloys possess excellent balance of mechanical properties. The first generation of Ti_2AlNb based alloys are Ti-25Al-17Nb and Ti-22Al-23Nb, and in the early 1990s, the second generation of Ti_2AlNb based alloy Ti-22Al-27Nb was developed and has been patented[5]. It is found that the mechanical properties of Ti_2AlNb based alloys depend on microstructures. The equilibrium of Ti-Al-Nb has shown that the phase combination of Ti_2AlNb based alloys are sophisticated[6,7], and this provides a possibility to secure optional mechanical properties balance by controlling the microstructure from thermal mechanical processing and heat treatment. In this paper, Nb in Ti-22Al-27Nb was partly substituted by Ta, and various combinations of thermal mechanical processing and heat treatment were investigated to control the microstructure of Ti-22Al-20Nb-7Ta. The tensile mechanical properties and fracture behaviors of this alloy was studied.

2 EXPERIMENTAL

Cast ingots of 250 g with a nominal composition of Ti-22Al-20Nb-7Ta were procured by magnetic-suspension melting technology. Composition of as-cast ingots was measured, and it was found that the actual composition is almost the same as the nominal one, and the oxygen content is lower than 5×10^{-4}%, the nitrogen content is lower than 6×10^{-5}%, the hydrogen content is lower than 4×10^{-5}%. The ingots were annealed at 1 200 ℃ for 24 h and then sealed in a stainless steel can followed by forging at 1 200 ℃ in air into rods with a diameter of 25 mm. According to the $B2$ transus temperature t_S, three kinds of combination of hot processing and heat treatment were designed.

HT1: The forged rod was rolled to 4 mm thick sheet at a certain temperature t_A in three phase zone ($O+\alpha_2+B2$), and followed by solution treatment above t_S, then 870 ℃ aging for 10 h, and water quenching.

① **Received date:** Apr.28, 1999; **accepted date:** Aug.20, 1999

HT2: The forged rod was solutionzed above t_S, followed by annealing at t_B for 2 h in two phase zone ($O+B2$), then water quenching. After heat treatment, the rod was rolled to 4 mm thick sheet at t_C in two phase zone ($O+B2$), and followed by heat treat ment at t_C for 2 h, and water quenching.

HT3: The forged rod was solution treated above t_S, followed by annealing at t_B for 2 h, then water quenched. After heat treatment, the rod was rolled to 4 mm thick sheet at t_A, followed by 800 ℃ annealing for 2 h, and water quenching.

The tensile specimens with 22 mm gage length were electro-discharged from the heat treated rolled sheets. Tensile tests were performed on a MTS-810 machine at room temperature in air, and the crosshead speed was 0.5 mm/min. After fracturing, fractographs were observed by SEM. The constituent phases were studied by XRD.

3 RESULTS AND DISCUSSION

3.1 Microstructure

Fig.1 shows the back scattered elctron images of Ti-22Al-20Nb-7Ta alloy with different processing combinations. According to Nb content in constitutent phases, the dark contrast is α_2, the bright contrast is $B2$ phase, and the gray contrast is O phase. Fig.1(a) shows the back scattered electron image of Ti-22Al-20Nb-7Ta with HT1. It is shown that after being treated by HT1, $B2/\beta$ solution grain boundaries remained, and α_2 grain did not resolve completely. The dominate microstructure was laths of $B2+O$ and equiaxed α_2 grains. Fig.1(b) shows the back scattered electron image of Ti-22Al-20Nb-7Ta with HT2. O phase grain became equiaxed, and some O phase grains remained elongated. By HT2, the principal microstructure was fine equiaxed O phase grain in $B2$ matrix. Fig.1(c) shows the back scattered image of Ti-22Al-20Nb-7Ta with HT3. A small volume of equiaxed α_2 grains was dispersed in lath mixture of $O+B2$, but there was no $B2/\beta$ solution grain boundaries remained, and the size of laths of O and $B2$ is finer than that with HT1.

Fig.2(a) and Fig.2(b) show the XRD results of Ti-22Al-10Nb-7Ta with HT1 and HT2, respectively. It is shown that this alloy is constituted of three phases, α_2+B2+O after treated by HT1, while two phases, $O+B2$ after treated by HT2. The isopleth of Ti-23Al/Nb was presented in Ref.[8] by Bendersky et al. From Boehlert and Majumdar[9], for Ti-23Al-27Nb, the $B2$ transus temperature is 1 070 ℃, three phases zone (α_2+B2+O) is located in the range of 1 070 ~ 1 010 ℃, α_2+B2 two phases zone located in 1 010 ~ 975 ℃, $O+B2$ two phases zone located in 975 ~ 870 ℃, and below 870 ℃, single O phase. Our results show that the transus temperature of Ti-22Al-20Nb-7Ta, t_S is 1 070 ℃. For HT1, the alloy was rolled at a temperature in three phases zone. The followed solution above t_S results in coarse $B2/\beta$ grains. Because of short duration of solution, α_2 resulted from rolling is not resolved completely, and following aging at 870 ℃ gives rise to precipitation of $B2+O$ laths. The prior $B2/\beta$ grain boundaries are the optional sites of precipitation, so Widmannstäntten microstructure was formed by HT1. For HT1 and HT2, prior to rolling, the microstructure of Ti-Al-20Nb-7Ta was uniform laths of $B2+O$. Rolling temperature located in different phase zones, different microstructures were obtained for HT1 and HT2.

3.2 Tensile properties and fracture behaviors at room temperature

Table 1 lists the tensile properties of Ti-22Al-

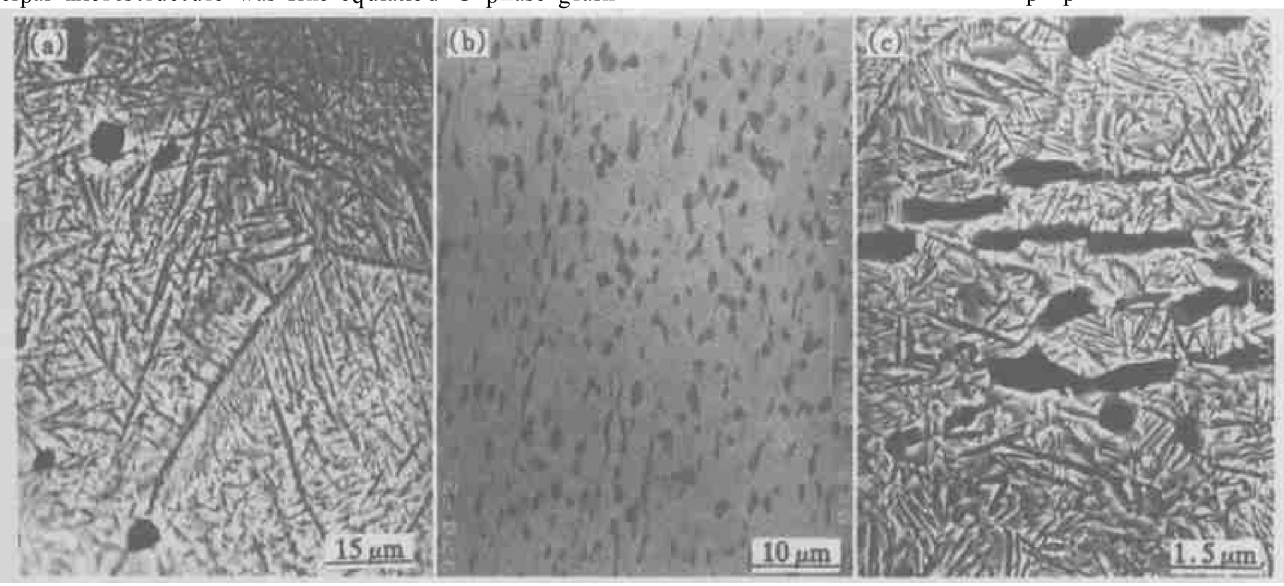

Fig.1 SEM back scattered electron images of Ti-22Al-20Nb-7Ta
(a) —With HT1; (b) —With HT1; (c) —With HT3

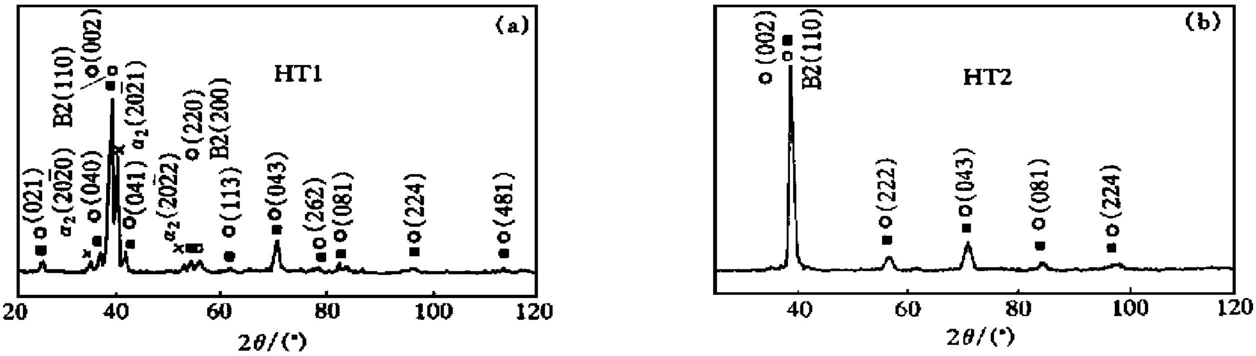

Fig.2 XRD patterns of Ti-22Al-20Nb-7Ta alloy
(a) —HT1 treatment; (b) —HT2 treatment

Table 1 Tensile properties of Ti-22Al-20Nb-7Ta at room temperature

Heat treatment	Microstructure	Average yield strength/MPa	Average ultimate strength/MPa	Elongation /%	Fracture mode
HT1	Lath of $O+B2$ with remained coarse β grain boundary and α_2 phase	910	965	3.6	Intergranular fracturing
HT2	Equiaxed O phase grain in $B2$ matrix	1 070	1 090	9.3	Transgranular fracturing
HT3	Fine lath of $O+B2$ without remained coarse β grain boundary	1 240	1 350	10.0	Transgranular fracturing

20Nb-7Ta alloy with different microstructures. From Table 1, strong dependence of mechanical properties upon microstructure is shown. The microstructure of fine laths of $O+B2$ without remaining coarse β grain boundaries secured by HT3 has the best tensile properties at room temperature so far. By HT1, the yield strength and elongation are the lowest for the microstructure of laths of $O+B2$ with remaining coarse β grain boundaries and α_2 phase. By HT2, the tensile properties are between those of HT1 and HT3. The tensile properties of various Ti-Al-Nb system alloys were reported in Ref.[10], and it is shown that the microstructure obtained by HT3 provided the best tensile properties for all Ti_3Al based alloys. Comparing Ti-22Al-20Nb-7Ta alloy with Ti-22Al-27Nb developed by Rowe, the former possesses better ductility at room temperature while has almost the same high yield stress as the latter, which is beneficial to its workability.

Fig.3 shows the fractographs of Ti-22Al-20Nb-7Ta alloy with different processing combinations. For HT1, the fracture mode of Ti-22Al-20Nb-7Ta alloy is intergranular fracturing, as shown in Fig.3(a). Fig.3(b) and 3(c) are fractographs for HT2 and HT3, respectively, and the fracture modes for them are mainly transgranular fracturing. The fracture modes of this alloy are correspondent to its microstructures. According to the Hall-Petch rule, the

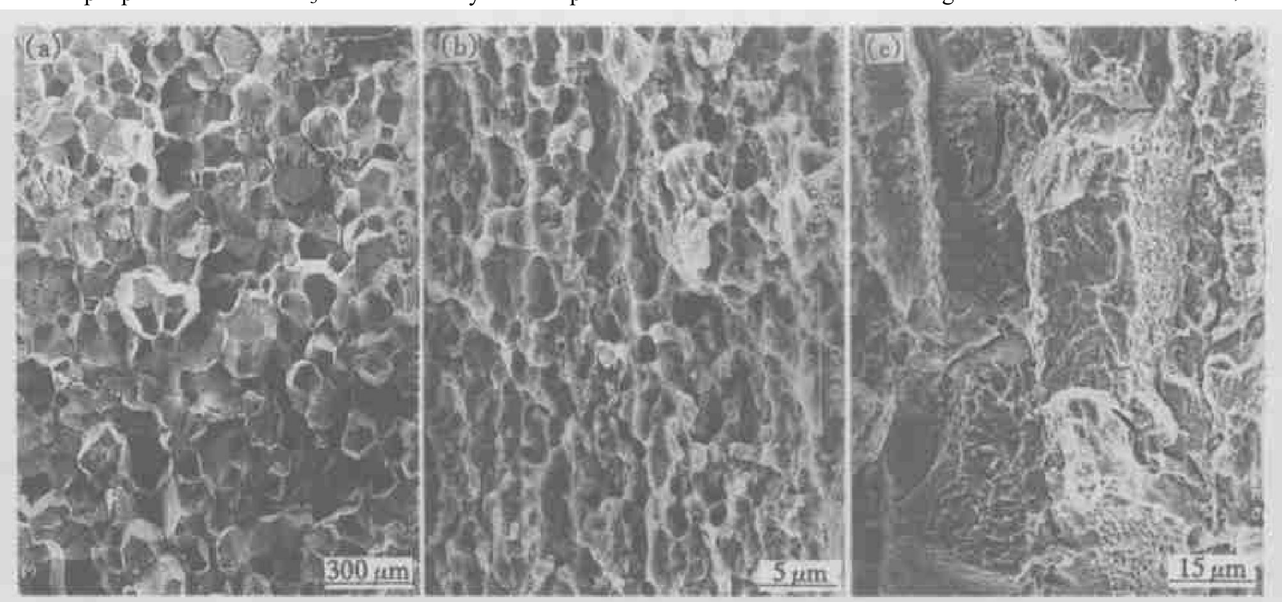

Fig.3 Fractographs of Ti-22Al-20Nb-7Ta
(a) —HT1 treatment; (b) —HT2 treatment; (c) —HT3 treatment

coarse $B2/\beta$ grain boundaries will deteriorate the yield strength and ductility at room temperature. The coarse $B2/\beta$ grain boundaries responsible for the intergranular fracturing. Because the distribution of impurity was not studied in this alloy, whether the impurity on grain boundaries is another responsible factor is not determined now, although Ta was distributed uniformly in Ti-22Al-20Nb-7Ta. Considering the tensile properties and microstructures for HT2 and HT3, the tensile properties of Ti-22Al-20Nb-7Ta are correspondent not only with the volume fraction of the constitutent phases, but also with the phase forms. However, which is the dominant factor is not determined now. According to the mixture rule of composite, the yield stress of this alloy can be formulated as $\sigma_a = \sigma_O f_O + \sigma_{B2} f_{B2}$, while σ_O and σ_{B2} are the yield stress of O and $B2$ phases respectively, and f_O and f_{B2} are the volume fractions of O and $B2$ phases, respectively. This formula leads to optimized tensile properties of Ti_2AlNb based alloys by controlling their microstructure.

4 CONCLUSIONS

1) The tensile mechanical properties of Ti_2AlNb based alloys were affected by their microstructures severely. The microstructure of fine laths of $O+B2$ without remaining coarse β grain boundaries secured by HT3 had the best tensile properties at room temperature so far. The yield strength is 1 240 MPa, and elongation is 10 %.

2) The fracture mode was contributed to the remaining coarse β grain boundary. For the microstructure of laths of $O+B2$ with remaining coarse β grain boundaries and α_2 phase, the fracture mode was intergranular, while for the other two microstructures without remaining coarse β grain boundaries, the fracture mode was transgranular.

REFERENCES

[1] Satry S M L and Lipsitt H A. Ordering transformations and mechanical properties of Ti_3Al and Ti_3AlNb alloys [J]. Metall Trans, 1997, 8A(10): 1543.

[2] Dimiduk D M, Miracle D B and Ward C H. Development of intermetallic materials for aerospace system [J]. Mater Sci and Tech, 1992, 8(4): 367.

[3] Rowe R G. Advanced Ti_3Al-base alloy property comparison [J]. Key Eng Mater, 1993, 77 ~ 78: 61.

[4] ZHONG Z, ZOU D and LI S. Advance in Ti_3Al and TiAl intermetallics research in CISRI [J]. Acta Metallurgica Sinica (English letters), 1995, 8(4 ~ 6): 534.

[5] Rowe R G. US 5032357. 1991.

[6] Muraaleedhran K, Gogia A K, Nandy T K, et al. Transformation in a Ti-24Al-15Nb alloy: Part I. phase equlibria and microstructure [J]. Metall Trans, 1992, 23A: 401.

[7] Kumpfert J and Leyens C. Microstructure evolution phase transformation and oxidation of an orthorhomobic titanium aluminide alloy [A]. Nathal M V, Liu C T, Martin P L, et al. Structural Intermetallics 1997 [C]. MMRS, 1997. 895.

[8] Bendersky L A, Boettinger W J and Roytburd A. Coherent precipitates in the BCC/orthorhombic two-phase field of Ti-Al-Nb system [J]. Acta Metallurgica Materials, 1991, 34: 1005.

[9] Boehlert C J, Majumdar B S, Seetharaman V, et al. Phase evolution, stability, and microstructure-creep relations in orthorhombic Ti-23Al-27Nb alloy [A]. Nathal M V, Liu C T, Martin P L. Stuctural Intermetallics 1997 [C]. MMRS, 1997. 795.

[10] Banerjee D. Chapter 5: Ti_3Al and its alloys [A]. Westbrook J H and Fleischer R C. Intermetallics Compounds [C], 1994. 91.

(Edited by PENG Chao-qun)